Citation: Molecular Therapy — Methods & Clinical Development (2016) **3,** 15055; doi:10.1038/mtm.2015.55
Official journal of the American Society of Gene & Cell Therapy

www.nature.com/mtm

ARTICLE

AAV9-mediated central nervous system–targeted gene delivery via cisterna magna route in mice

Vera Lukashchuk[1], Katherine E Lewis[1], Ian Coldicott[1], Andrew J Grierson[1] and Mimoun Azzouz[1,2]

Current barriers to the use of adeno-associated virus serotype 9 (AAV9) in clinical trials for treating neurological disorders are its high expression in many off-target tissues such as liver and heart, and lack of cell specificity within the central nervous system (CNS) when using ubiquitous promoters such as human cytomegalovirus (CMV) or chicken-β-actin hybrid (CAG). To enhance targeting the transgene expression in CNS cells, self-complementary (sc) AAV9 vectors, scAAV9-GFP vectors carrying neuronal Hb9 and synapsin 1, and nonspecific CMV and CAG promoters were constructed. We demonstrate that synapsin 1 and Hb9 promoters exclusively targeted neurons *in vitro*, although their strengths were up to 10-fold lower than that of CMV. *In vivo* analyses of mouse tissue after scAAV9-GFP vector delivery via the cisterna magna revealed a significant advantage of synapsin 1 promoter over both Hb9 variants in targeting neurons throughout the brain, since Hb9 promoters were driving gene expression mainly within the motor-related areas of the brain stem. In summary, this study demonstrates that cisterna magna administration is a safe alternative to intracranial or intracerebroventricular vector delivery route using scAAV9, and introduces a novel utility of the Hb9 promoter for the targeted gene expression for both *in vivo* and *in vitro* applications.

Molecular Therapy — Methods & Clinical Development (2016) **3**, 15055; doi:10.1038/mtm.2015.55; published online 17 February 2016

INTRODUCTION

Gene therapy research relies on the use and optimization of safe nonreplicating viral vectors. The choice of the viral vector depends on the tropism of the virus and its ability to allow sustained therapeutic gene expression in the target cells. A key challenge to be overcome when designing an efficient gene therapy approach for treating neurodegenerative disorders is access to the central nervous system (CNS), which must be mediated by either crossing the blood–brain barrier or by direct administration into the CNS. Adeno-associated virus of serotype 9 (AAV9) has become a preferred vector for CNS delivery, due to its increased ability to cross the blood–brain barrier compared to other AAV serotypes.[1,2] Indeed, several studies have demonstrated successful reversal of the disease phenotype and prolonged survival in mouse models of spinal muscular atrophy and amyotrophic lateral sclerosis upon intravenous AAV9 delivery.[3–5] However, complications from systemic delivery of AAV9 and its expression in non-CNS tissues such as liver and heart are likely barriers to their success in patient clinical trials.[6–9] Delivery into the cerebrospinal fluid via intracerebroventricular route provides some protection against diffusion of the AAV9 vector to peripheral organs and more efficiently targets neurons and glia.[10] Similarly, cisterna magna route of injection has been recently adopted as an alternative method for delivery into cerebrospinal fluid (CSF) which results in wide-spread gene delivery throughout the CNS[11–16]; however, the data regarding the therapeutic efficacy using this administration route in mouse models is sparse. The findings reported here aim to improve the therapeutic potential of the AAV vectors when targeting to the motor neurons and motor pathways within CNS.

We previously demonstrated that the delivery of scAAV9 expressing *survival motor neuron* (SMN, causative gene for spinal muscular atrophy) driven by human cytomegalovirus (CMV) promoter into neonatal mice fully rescues early lethality in mice.[5] Using self-complementary (sc) AAV9 ensures a faster rate of gene transcription onset due to the double-stranded conformation of the genome unlike conventional recombinant AAVs.[17] The CMV promoter is known to drive high levels of gene expression across both CNS and non-CNS tissues when used in AAV vectors, and is therefore not necessarily an ideal promoter to use for restricted CNS transduction.[10,18,19] Several neuronal promoter sequences, including synapsin 1, CamkII, MeCP2, and Hb9 have been previously used to restrict gene expression to the spinal cord and brain using viral vectors.[20–26] Efficient gene expression in the motor neurons of lumbar spinal cord was achieved after intracerebroventricular injection of mice using AAV9 driven by synapsin 1.[10,20] Hb9 is a motor neuron-specific promoter whose activity has been well-established in the developing and postnatal spinal cord.[27,28] In addition to motor neurons, a subset of Hb9-positive spinal cord interneurons has also been reported.[29] Two short regulatory sequences within the distal region of Hb9 promoter with a size of 313 and 125 base pairs have been identified as sufficient for targeting gene expression exclusively to spinal cord in transgenic embryonic mice.[30] While lentiviral vectors expressing Hb9 enhancer-driven green fluorescent protein

[1]Sheffield Institute for Translational Neuroscience, Department of Neuroscience, University of Sheffield, Sheffield, UK; [2]Faculty of Applied Medical Sciences, King Abdulaziz University, Jeddah, Saudi Arabia. Correspondence: M Azzouz (m.azzouz@sheffield.ac.uk)
Received 30 July 2015; accepted 9 December 2015

(GFP) resulted in moderate gene transfer efficiencies after intraparenchymal injection directly into the ventral horn of the lumbar spinal cord,[26] expression data from AAV vectors driven by Hb9 have not been reported.

In the present study, we sought to assess the neuron-targeting properties and transduction efficiencies of scAAV9-GFP vectors carrying the Hb9 promoter enhancer elements and synapsin 1 (SYN1) promoter after delivery of the virus into neonatal mice via the cisterna magna by comparing them to the ubiquitous promoters CMV and chicken-β-actin fused to CMV enhancer (CAG). Our results demonstrate the first account on the use of promoters of varying strengths and specificities in scAAV9-mediated reporter GFP expression after intra-CSF delivery via cisterna magna in mice. In addition, they highlight the novel applicability of the promoter Hb9 in therapeutic gene transfer to areas of the brain stem.

RESULTS

Characterization of scAAV9-GFP vectors carrying neuronal promoters in spinal cord neurons *in vitro*

One of the challenges associated with constructing a transgene within scAAV genomes is their small cloning capacity. Despite this, several studies have demonstrated efficient neuronal targeting using a short ~400 bp SYN1 promoter sequence[20,22,25] while Hb9 promoter enhancer elements[30] have never previously been tested in AAV delivery systems. In this study, we assessed the activities of SYN1 and Hb9 hybrid promoters in a side-by-side comparison to conventionally used CAG and CMV promoters, which are known for their high-level ubiquitous expression properties. Five scAAV9-GFP virus stocks carrying different promoter elements including CMV, CAG, Hb9 enhancer composed of two minimal Hb9 promoter sequences (Hb9e), Hb9 enhancer fused to CMV minimal promoter (Hb9cmv) and SYN1 (Figure 1) were produced to high titers (up to 3×10^{13} vg/ml). Spinal cord cultures purified from embryonic day 13 (E13) mouse embryos, containing motor neurons and interneurons as well as glia, were transduced on day *in vitro* 2 and analyzed after 7 days. Representative image fields of the transduced cells used in quantification analyses are shown in Figure 2a. Promoter activities were determined by two principal measures: (i) the percentage of GFP-positive cells (transduction efficiency; Figure 2b) and (ii) the fluorescence intensity of the GFP-positive cells (promoter strength; Figure 2c). Cells transduced with CMV and CAG viral vectors resulted in the majority of the cells expressing GFP (97 and 82%, respectively), while the transduction with the viral vectors encoding neuronal promoter constructs Hb9cmv, SYN1, and Hb9e resulted in a lower proportion of GFP-positive cells (59, 58, and 19%, respectively; Figure 2b). The Hb9e vector resulted in significantly lower ($P < 0.0001$) transduction levels than those with other promoters. Analysis of the GFP intensity signal in the transduced cells revealed that despite similarities between CAG and CMV promoters in cell-targeting efficiencies, CAG promoter strength was almost threefold lower than that of CMV (Figure 2c). It was evident that in the case of Hb9, the short CMV minimal promoter significantly enhanced gene expression ($P < 0.01$). Interestingly, in this *in vitro* assay, SYN1 had a comparably low strength to Hb9e construct (~50 intensity units; Figure 2c), despite having achieved 58% average gene transfer efficiency as demonstrated in Figure 2b.

Both synapsin 1 and Hb9 target neurons, but not astrocytes, *in vitro*

In order to confirm the specificity of the promoter elements constructed in this study, the cell types targeted by SYN1 and Hb9 promoters were analyzed by immunocytochemistry using cell-type specific markers. scAAV9-CMV and scAAV9-CAG transduction resulted in high transduction efficiency within both neurons and astrocytes, visualized by staining with the pan-neuronal marker MAP2 and the astrocytic marker glial fibrillary acidic protein (GFAP), respectively (Figure 3a–d). Consistent with their neuronal origin, SYN1, Hb9cmv and Hb9e promoters were driving strictly neuronal gene expression (Figure 3e–j), as determined by distinctive neuronal morphology and a lack of double-GFP/GFAP-positive cells. Surprisingly, transduction with Hb9cmv vector did not result in GFP expression in GFAP-positive or MAP2-negative cells, despite the presence of the CMV minimal promoter normally associated with ubiquitous expression (Figure 3g–h). Immunostaining for motor neuron marker Islet-1 (Supplementary Figure S1) revealed that motor neurons were efficiently targeted by all promoter constructs, suggesting the utility of these vectors in *in vitro* applications when neuronal tropism is required.

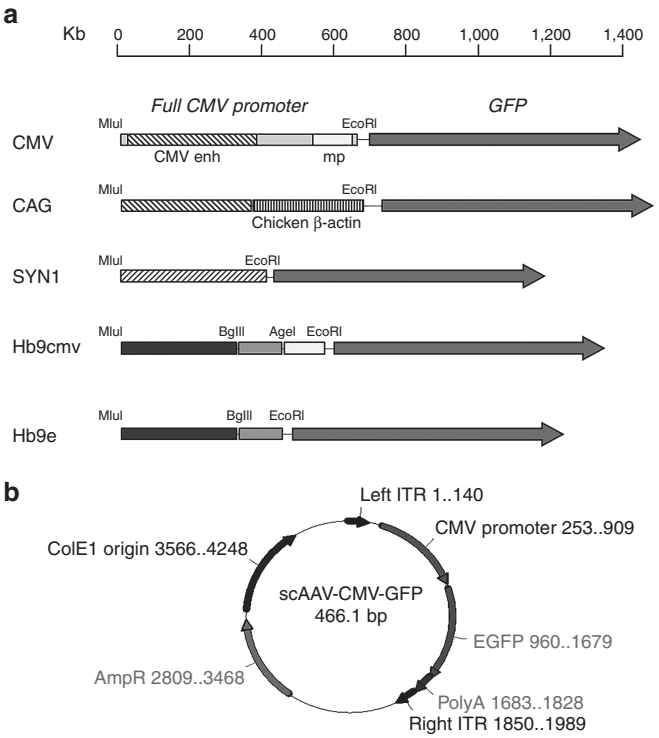

Figure 1 Construction of scAAV-GFP plasmids with neuronal promoter/enhancer elements. Schematic representation of the scAAV9 vectors utilized in this study. Promoter elements were polymerase chain reaction-amplified from corresponding plasmids (see Materials and Methods), introducing appropriate restriction sites depicted in (**a**). The entire promoter fragments were cloned between *Mlu*I and *Eco*RI restriction sites and inserted into scAAV-GFP plasmid (**b**). A representative vector containing full CMV promoter is shown in (**b**).

Synapsin 1 promoter, but not Hb9, results in low to moderate targeting of gene expression to motor neurons of the spinal cord

In order to assess *in vivo* gene transfer applicability of SYN1 and Hb9 promoters in comparison with the conventionally used CMV and CAG in scAAV9 vectors *in vivo*, postnatal day 1 wild-type mice (n = 3 per group) were injected via the cisterna magna with 1×10^{10} viral genomes of five titer-matched scAAV9-GFP vectors harboring CMV, CAG, SYN1, Hb9cmv, and Hb9e promoter sequences. CNS tissue was paraformadehyde (PFA)-perfused and harvested for immunohistochemistry analyses at 3 weeks postinjection. Immunostaining

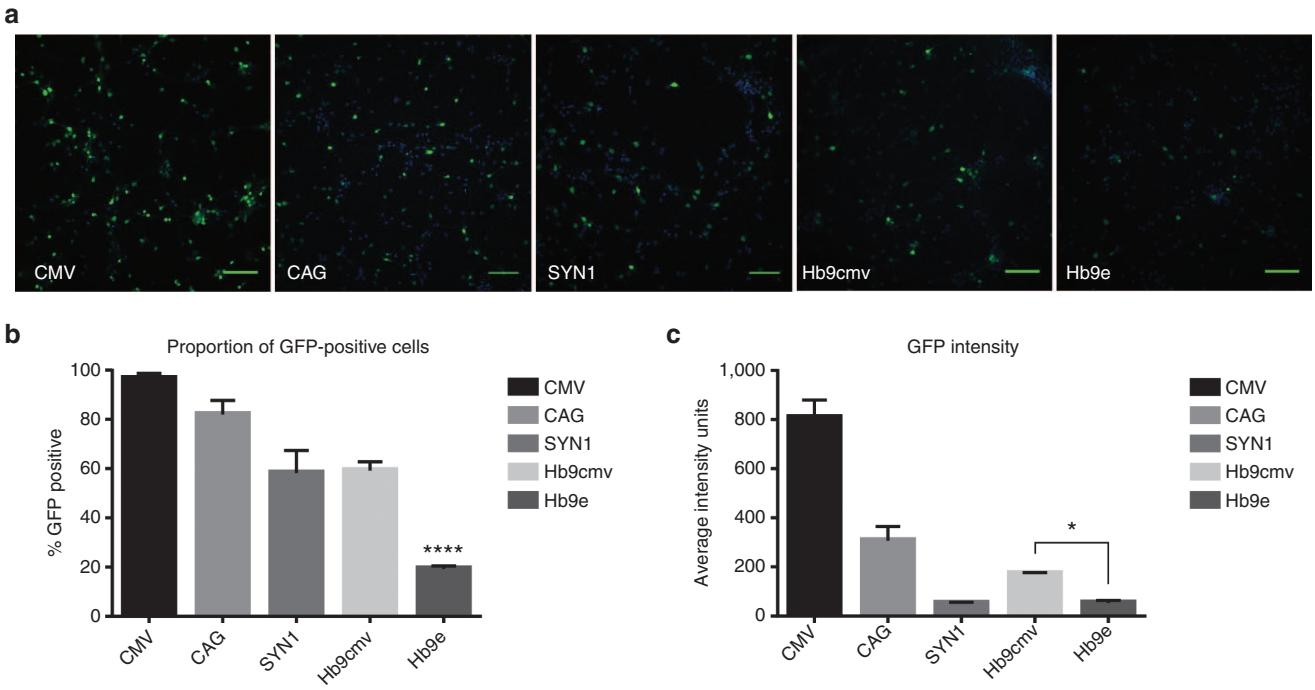

Figure 2 Activity of the promoter constructs in scAAV9-GFP in embryonic mouse spinal cord culture. Mixed spinal cord culture was established from E13 wild-type mouse spinal cords. Cells were transduced with indicated virus at 2 days *in vitro* and fixed at 7 days post-transduction. GFP-positive cell numbers and the fluorescence levels were quantified using automated InCell Developer software. For establishing statistical significance, one-way analysis of variance test was used with Tukey's multiple comparison test; *$P < 0.01$, ****$P < 0.0001$. (**a**) Representative images used in quantification by InCell Developer software. (**b**) *In vitro* transduction efficiency of scAAV9-GFP constructs measured as a proportion of the GFP-positive cells/nuclei of the total Hoechst-positive nuclei. (**c**) Promoter activities were determined as fluorescence intensities. Y axis represents average grey levels measured in each GFP-positive cell normalized to background. Bar graphs represent mean ± SD ($n = 3$). Scale bar = 100 µm.

of the spinal cord sections with anti-NeuN antibody has demonstrated efficient CNS-targeting capacities of CMV, CAG, and SYN1 but not Hb9cmv or Hb9e promoters when used at the same dose (Supplementary Figure S2; Figure 4). In the spinal cord, scAAV9-CMV-GFP transduction resulted in the highest GFP-positive cell numbers and most intense fluorescence levels in both the lumbar and cervical regions (Figure 4a,i), while CAG and SYN1 were noticeably weaker promoters (Figure 4c,e—lumbar cord; k,m—cervical cord). Moreover, unlike CMV (Figure 4b,j), SYN1 targeted CGRP-positive motor neurons within the lumbar spinal cord with lower efficiency (Figure 4f,h). Surprisingly, none of the ventral horn neurons of the animals treated with scAAV9-Hb9cmv and scAAV9-Hb9e expressed GFP (data not shown), although several GFP-positive interneurons (up to 10 per area) were detected within the dorsal horns of the lumbar spinal cord (Figure 4g).

Quantification of the GFP-positive cells in each region, from three spinal cord sections located approximately 250–300 µm apart (Figure 4o), revealed that indeed CMV promoter-driven expression resulted in significantly higher ($P < 0.0001$) relative GFP-positive numbers of cells within cervical spinal cord, but not within lumbar spinal cord, when compared to CAG and SYN1. Analysis of the CGRP-positive motor neurons within the cervical and lumbar spinal cord (Figure 4p) determined a transduction efficiency of about 80% for motor neurons in CMV-treated animals. Transduction with both scAAV9-CAG and scAAV9-SYN1 across the spinal cord resulted in a significantly lower proportions of GFP-positive/CGRP-positive motor neurons than with CMV. These findings demonstrate that the CMV promoter has a distinct advantage for spinal cord gene transfer, particularly to motor neurons, over both SYN1 and CAG promoters when the vectors are delivered intracisternally.

Cisterna magna delivery of scAAV9 virus allows efficient transduction throughout the mouse brain

Determining the areas of the brain targeted by various promoters can identify therapeutically relevant promoters for gene delivery to treat neurological disorders. Here, we analyzed four principal areas of the brain after transduction with CMV, CAG, SYN1, Hb9cmv, and Hb9e promoter-bearing scAAV9-GFP viral vectors delivered through cisterna magna: cerebellum, motor cortex, motor-related areas of the brain stem, and hippocampus (Figure 5; Supplementary Figure S3). Merged-view representative images of the brain sections immunostained with anti-NeuN and anti-GFP antibodies provided qualitative information about the overall distribution and the levels of transgene expression. As expected, CMV and CAG were very efficient at targeting gene expression throughout the brain. SYN1 showed a uniform distribution of the GFP-positive neurons throughout the brain (Figure 5 and Supplementary Figure S3). Interestingly, Hb9cmv and Hb9e promoter constructs were driving GFP expression in the brain stem, with majority of the GFP-positive cells detected around the motor and sensory areas of the midbrain (Figure 5b). Upon a closer inspection, the areas positive for GFP in Hb9cmv-treated animals were identified as motor-related areas of pons such as tegmental reticular nucleus and midbrain reticular nucleus. We also observed high frequency of GFP-positive cells in sensory areas of midbrain including superior and inferior colliculi. Unlike Hb9cmv, Hb9e did not mediate expression in the sensory areas, but still showed expression predominantly within the periaqueductal gray and tegmental areas, as seen in the low-magnification image in the Supplementary Figure S3. All promoters except Hb9e were capable of driving GFP expression within the cerebellum, predominantly within the Purkinje cell layer (Figure 5a). Purkinje cells

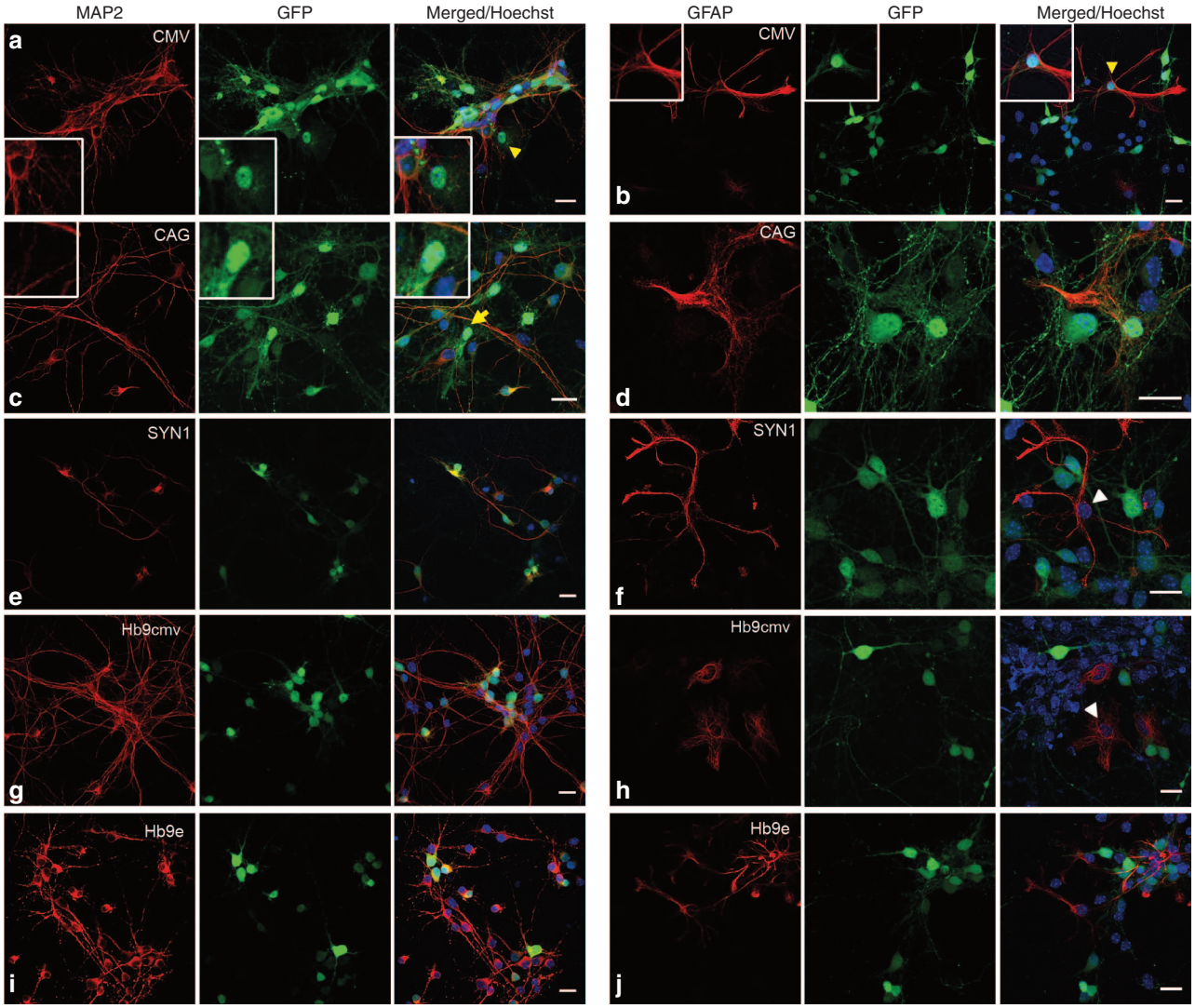

Figure 3 scAAV9-GFP carrying neuronal promoters transduce spinal cord neurons *in vitro*. Mixed spinal cord culture was established from E13 mouse embryos. Transduced spinal cord cells were fixed at 7 days post-transduction and processed for immunocytochemistry using antibodies against neuronal tubulin marker MAP2 (**a, c, e, g, i**) and astrocytic marker GFAP (**b, d, f, h, j**). GFP signal was autofluorescence. (**a,b**) CMV, (**c,d**) CAG, (**e,f**) SYN1, (**g,h**) Hb9cmv, (**i,j**) Hb9e. Insets in (**a–c**) correspond to cells indicated by a yellow arrow head. White arrow heads indicate GFP-negative GFAP-positive astrocytes. Scale bar = 20 µm.

were identified by a distinct branched morphology, with their cell bodies located at the edge of granular cell layer. Hippocampus (particularly neurons of the polymorph layer within the dentate gyrus) and cerebral cortices were efficiently transduced with scAAV9 vectors carrying CMV, CAG, and SYN1 promoters, but were less efficiently transduced by Hb9cmv and Hb9e (Figure 5c,d); however, several detected GFP-positive cells suggested these Hb9 promoter constructs may have gene expression capabilities in these areas when delivered at higher doses.

Quantification of the GFP-positive cells within the chosen brain regions revealed similarities between the targeting properties of CMV, CAG, and SYN1 promoters across all four areas (Figure 5e–h). Hb9cmv and Hb9e promoters were significantly less efficient in transduction across cortex, hippocampus, and cerebellum, when normalized and compared to CMV. However, their transduction efficiencies within the brain stem (motor-related areas of midbrain; Figure 5g) were similar to those observed in the CMV-treated animals.

In order to account for the cell-type differences between the two conventionally-used promoters CMV and CAG, proportions of glial cells positive for GFP were determined, as a percentages of the total GFP-positive cell numbers represented (Supplementary Figure S4). Interestingly, we noticed that the number of transduced glia increased with the further location of the CNS areas from the injection site, with the highest proportions of GFP-positive cells located within lumbar cord region in animals injected with CMV or CAG vectors. GFP-positive glial cells were detected within the midbrain of Hb9cmv and Hb9e treated animals (Figure 5b, yellow arrow) and equaled 2.2 and 7.5%, respectively, and 8% within the motor cortex of Hb9cmv-treated animals, but were not included in the analysis presented in Supplementary Figure S4.

In summary, our study demonstrated that CMV, CAG and SYN1 have a significant advantage over Hb9cmv and Hb9e promoter activities when used in scAAV9-GFP vector system for transducing CNS in all of the regions tested, apart from the brain stem. Importantly, we have identified selective specificity of Hb9 enhancer for the brain

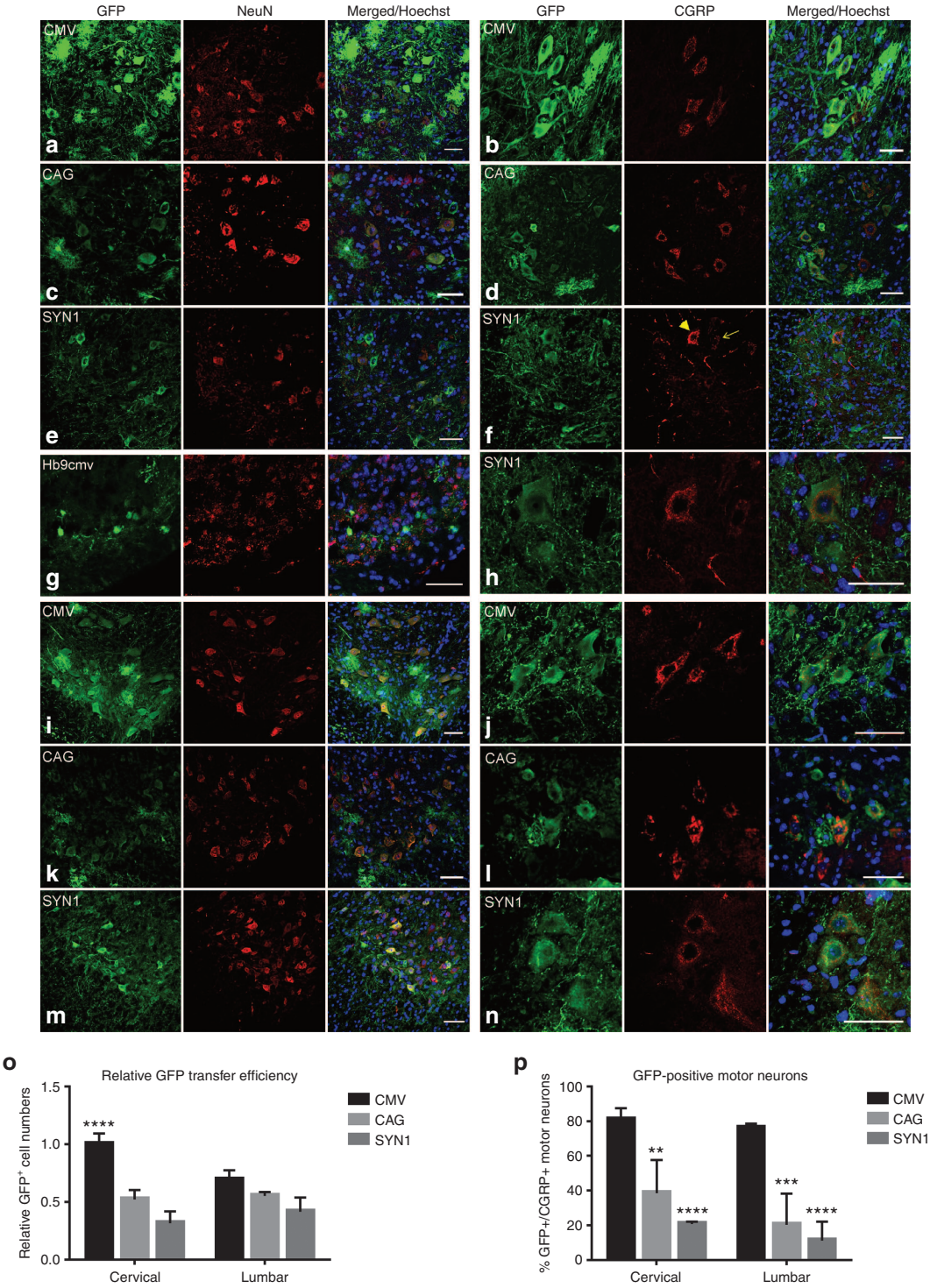

Figure 4 Intracerebrospinal fluid delivery via cisterna magna of scAAV9-GFP results in differential gene delivery efficiencies in the mouse spinal cord depending on the use of the promoter. Wild-type mice at postnatal day 1 were injected with different scAAV9 viral vectors at equal doses of 1×10^{10} vg/g and sacrificed after 21 days post-transduction. Lumbar spinal cord (**a–h**) and cervical spinal cord (**i–n**) 25 µm sections were immunostained with anti-GFP and anti-NeuN (left set of panels) or anti-CGRP antibodies (right set of panels), as indicated. (**a,b**), (**i,j**)—CMV; (**c,d**), (**k,l**)—CAG; (**e,f**), (**h**), (**m,n**)—SYN1; (**g**)—Hb9cmv. For SYN1-transduced ventral horn, a representative field with GFP-negative CGRP-positive motor neurons (**f**, arrow) as well as a less frequently occurring GFP-positive CGRP-positive motor neuron (**h**; a higher magnification image of the GFP-positive motor neuron denoted by an arrowhead in panel **f**) are shown. (**g**) Representative image of Hb9cmv-treated animal demonstrates GFP-positive lumbar cord dorsal horn interneurons. Scale bar = 50 µm. *In vivo* transduction efficiency (**o**) was determined based on the total numbers of GFP-positive cells within three ventral horns of cervical and lumbar regions, and normalized to the average CMV numbers in the cervical spinal cord region. Percentage of the motor neurons double-positive for CGRP/GFP (**p**) demonstrate the efficiency of the motor neuron targeting within the spinal cord regions. Hb9cmv and Hb9e were omitted from the graphs (**o,p**) due to the lack of detectable GFP-positive fluorescence. The results were analyzed using two-way analysis of variance followed by Tukey's test for multiple comparisons. $^{**}P < 0.01$; $^{***}P < 0.001$; $^{****}P < 0.0001$. Bar graphs represent mean ± SD ($n = 3$).

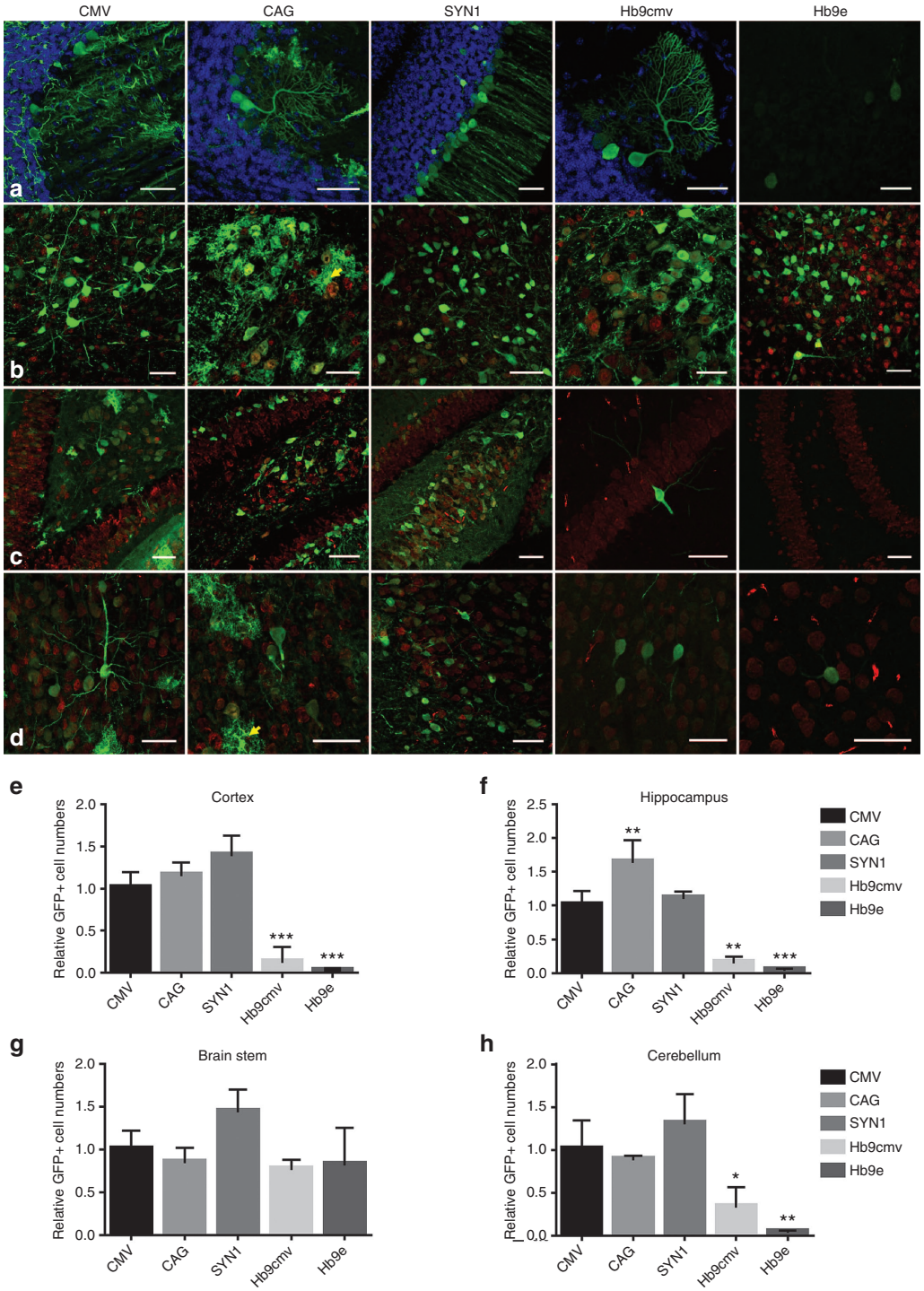

Figure 5 GFP expression in the brain following cisterna magna delivery of scAAV9-GFP vectors with different promoters. 40-µm brain sections of 3-week-old transduced and PFA-perfused mice were immunostained with anti-GFP and anti-NeuN antibodies (**b–d**), or with anti-GFP antibodies alone (**a**) for NeuN-negative Purkinje neurons of the cerebellum (Hb9e treatment shown with anti-GFP antibody staining only, to avoid masking the weak GFP signal). Representative images were captured on the sections of cerebellum (**a**), brain stem (midbrain, motor-related; **b**), hippocampus (dentate gyrus—polymorph layer; **c**), and motor cortex (**d**). Yellow arrow heads point to NeuN-negative glial cells used in quantification (determined by morphology). Scale bar = 50 µm. Efficiency of transduction in the brain was determined by counting GFP-positive cells in 1 mm^2 area of each brain section and normalizing the resulting numbers to the average number of CMV treatment for each brain region (**e**—cortex; **f**—hippocampus; **g**—brain stem; **h**—cerebellum). The bar graphs represent relative mean ± SD. Statistical significance was determined using one-way analysis of variance with Bonferroni test for multiple comparisons normalized to a control CMV. *$P < 0.05$; **$P < 0.01$; ***$P < 0.001$; ****$P < 0.0001$.

stem region, particularly those areas involved in the motor control pathways, when scAAV9-Hb9-GFP vectors were delivered via cisterna magna.

DISCUSSION

Previous reports have demonstrated the ability of scAAV9 vectors to cross the blood–brain barrier when delivered intravenously.[2,31] Direct administration of scAAV9 to the CSF, coupled with the use of a specific promoter, can further target desired cell types within the CNS and is of particular interest to neurodegeneration therapeutics, where cell-specific expression of a transgene may be required. In this study, we examined transduction efficiency of cisterna magna-delivered scAAV9 expressing GFP under the control of neuron-specific SYN1, Hb9 enhancer (Hb9e), or Hb9cmv fusion promoters, and compared this to the ubiquitous CMV and CAG promoters. We have achieved widespread gene delivery throughout the brain and spinal cord by delivering scAAV9-GFP into cisterna magna of neonatal mice. We have demonstrated that the level of gene expression was dependent on the choice of the promoter. The current study revealed that Hb9 promoter regulatory sequences derived from the promoter of a motor neuron-specific gene were able to target expression to the areas of the brain stem, but not the spinal cord, while SYN1 promoter offered a uniform neuron-specific transduction throughout the CNS. The latter finding was consistent with previous studies using alternative AAV delivery routes.[10,20] Moreover, we demonstrate the novel applicability of the short Hb9 promoter elements for *in vitro* applications using AAV9 in primary neuron cultures for specific neuronal targeting, where moderate gene expression levels may be required.

Intracerebrospinal fluid delivery of AAV vectors via cisterna magna is a relatively recently established route of delivery in gene transfer studies, which has been gaining preference particularly in preclinical studies using large animals.[11–14] Major advantages of this delivery route include: (i) substantially smaller quantity of the vector required compared to systemic delivery of AAV vectors, which directly impacts standard laboratory production of multiple vector constructs and large-scale clinical-grade production of the virus; and (ii) reduction of viral particles reaching peripheral organs such as liver.[13,16] Recently published evidence suggests that AAV9, but not AAV1 or -5, expressing GFP under the control of the CMV promoter and delivered via cisterna magna leads to the most abundant transduction within the cervical and lumbar spinal cord regions of mice.[11] Consistent with these previous findings, here we observed efficient gene transfer in the brain and spinal cord of young mice, covering cerebellum, brain stem, hippocampus, and cortices using CMV, CAG, and SYN1 promoters. These data show that delivery of scAAV9 into the cisterna magna of neonatal mice is an efficient delivery route for widespread transduction of CNS regions.

Despite bypassing the blood–brain barrier, cisterna magna route of delivery does not offer neuron-specific gene expression due to the ability of AAV9 to infect a wide range of cells, an observation supported by our study and previous reports.[11,15,16] Given the implication of astrocytes in the pathology of neurodegenerative diseases, such as Alzheimer's disease, spinal muscular atrophy and amyotrophic lateral sclerosis,[32–35] the high level of non-neuronal cell transduction with CMV and CAG promoters, demonstrated in this study (Supplementary Figure S4), may be advantageous for those disease models. However, when there is a risk of disseminated expression of a protein with a potentially toxic function in off-target cell types and organs, neuron-specific promoters are preferred. Hb9cmv and Hb9e promoters, in addition to the well-characterized SYN1 promoter,[10,20–22] may provide such utility for the AAV9-mediated therapy targeting neurological diseases, as they confer minimal non-neuronal gene expression when used with scAAV9 background.

Hb9 protein is a transcription factor whose functions have been largely attributed to the spinal cord and, in particular, motor neurons.[28] Hb9 protein is a known motor neuron marker for neurons differentiated from induced pluripotent stem cells[36,37]; however, its role in the brain is not clearly defined. Our results provide novel information regarding the activity of the distal enhancer elements of Hb9 promoter within the brain stem of postnatal animals, suggesting that scAAV9-Hb9 could be a useful vector for directing gene expression selectively to brain stem neurons. However, the virtual lack of transduction by the Hb9 distal enhancer elements (Hb9e) at other CNS sites suggests that this selectivity would be gained at the expense of lower overall expression. While we cannot yet speculate about the complete lack of activity of these Hb9 enhancers in adult animals, given their weak expression *in vitro* (Figure 2), Hb9-driven GFP expression in living mice may also be below detection thresholds due to the vector doses used in our studies. The presence of GFP in the spinal cord driven by other promoters suggests that the absence of transduction with the Hb9 promoters in the spinal cord (Figure 4) was not due to inadequate delivery following cisterna magna administration. Interestingly, Peviani *et al*.[26], have previously reported astrocytic and other non-neuronal cell targeting using the same Hb9 enhancer sequences in the lentiviral vector platform after intraparenchymal delivery directly to the lumbar spinal cord. Similarly, we also observed some scattered non-neuronal cell targeting within the brain using both Hb9cmv and Hb9e promoters in scAAV9 system, suggesting that this was not exclusively due to the presence of the CMVmp sequence. A 1.6 kb pair distal promoter region, comprising the two enhancers targeted exclusively neurons when delivered via a lentiviral vector into the spinal cord.[26] These data would suggest that additional sequence elements within the distal promoter may also contribute to neuronal specificity; however, due to the transgene packaging capacity limitation in scAAV vectors, using larger promoter fragments would result in inefficient gene transfer irrespective of the delivery route. Additional transcriptionally conserved regions within the proximal part of the Hb9 promoter have been identified[27] but their applicability in gene therapy vectorology is yet to be established. A more comprehensive analysis of Hb9 promoter activity and its expression in diseased neurons may be required to be able to speculate whether therapeutic gene delivery using Hb9 promoter would be appropriate for neurodegenerative conditions.

In summary, despite the cell-type specificity conferred by a neuronal promoter, gene therapy studies may need to take into account the desired levels of therapeutic protein expression, the route of delivery and the amount of virus being used. Several clinical trials are currently focusing on the surgical delivery of the vectors for neurodegenerative disease, such as anti-Batten's disease therapy using intracranial routes for AAV2-CLN2 administration; whereas intravenous delivery is now being adopted as the route of administering AAV9-SMN vector for spinal muscular atrophy treatment in the phase 1/2 trial, with the outcome of this study currently pending.[38] Through the intracisternal route of delivery it is possible to achieve a high level of therapeutic gene delivery throughout CNS without highly invasive surgical intervention. In addition, cisterna magna delivery offers an attractive advantage for viral vector administration due to substantial reduction of the disseminated gene transfer to the peripheral organs and evasion of the host immune

response.[13] Combining this approach with sufficient viral genomes and targeted promoter constructs will achieve desired specificity tailored to a particular therapeutic gene target. In this way, our study represents another step forward towards a targeted design of a gene delivery strategy using AAV9 vectors.

MATERIALS AND METHODS

Plasmid constructs

Plasmid scAAV-CMV-GFP was received from St. Jude Children's Research Hospital (Memphis, TN). To construct the scAAV-GFP transgene plasmid vectors carrying different promoters (Figure 1), the promoter elements were amplified as described below and depicted on Figure 1, using the primers specified in Table 1, and cloned into scAAV-CMV-GFP cassette replacing the original CMV promoter. To generate Hb9 enhancer (Hb9e) and Hb9cmv hybrid promoter fused to CMV minimal promoter (mp), Hb9 regulatory elements of 313 and 120 bp long[30] were amplified from pHb9-EGFP expression vector (Addgene plasmid 16275 (ref. 29); Addgene, Cambridge, MA) containing the full Hb9 promoter sequence and cloned between restriction sites as indicated in Figure 1a. Full CMV promoter and CMVmp were derived from pAAV-MCS (Stratagene, Stockport, UK). Human synapsin 1 promoter was amplified from pAAV-SYN1-RFP, a gift from Edward Callaway (Addgene plasmid 22907).[21] CAG promoter, composed of chicken β-actin promoter and CMV enhancer, was amplified from pCAGGS plasmid obtained from the Belgian Coordinated Collection of Microorganisms.[39] Standard cloning procedures for DNA extraction and production of the large-scale plasmids were followed using QIAGEN kits following the manufacturer's instructions.

Large-scale production of scAAV9

Stocks of scAAV9-GFP were produced by transfecting human embryonic kidney HEK293T cells and purifying using iodixanol gradient purification method. Briefly, HEK293T cells in 15 cm dishes were transfected with packaging plasmids pHelper (Stratagene; Stockport, UK), pAAV2/9 (kindly provided by J.Wilson, University of Pennsylvania) and one of the transgene plasmids scAAV-GFP at 2:1:1 ratio, respectively, using polyethylenimine (1 mg/ml) in serum-free Dulbecco's modified Eagle's medium. At 4 days post-transfection, supernatant containing cell-released virus was harvested, treated with benzonase (10 unit/ml; Sigma, Poole, UK) for 2 hours at 37 °C and concentrated to equal to approximately 24 ml using Amicon Ultra-15 Centrifugal 100K Filters (Millipore, Watford, UK). Iodixanol gradient containing 15, 25, 40, and 54% iodixanol solution in phosphate-buffered saline (PBS)/1 mmol/l MgCl2/2.5 mmol/l KCl and virus solution was loaded and centrifuged at 69,000 revolutions per minute for 90 minutes at 18 °C. After ultracentifugation, the virus fractions were visualized on a 10% polyacrylamide gel, stained using SYPRO Ruby (Life Technologies, Paisley, UK) according to the manufacturer's guidelines. The highest purity fractions (identified by the presence of the three bands corresponding to VP1, VP2, and VP3) were pooled and concentrated further in the final formulation buffer consisting of PBS supplemented with an additional 35 mmol/l NaCl[40] using Amicon Ultra-15 Centrifugal 100K filters. Viral titers were determined by quantitative PCR assays using primers directed against GFP and a linearized scAAV-CMV-GFP vector as a standard curve.

In vitro AAV transduction of the embryonic mouse spinal cord neurons

A pregnant female wild-type C57bl/6 mouse was sacrificed at 13 days of gestation (E13) using Schedule 1 method in accordance with Home Office UK regulations. Embryos were removed, and the spinal cords were dissected out. The cells were dissociated by trypsinization and trituration, pooled together and plated onto 10 mm glass coverslips precoated with 50 µg/ml poly-D-ornithine hydrobromide and 2.5 µg/ml laminin (Sigma, Poole, UK) at a density of 60,000 cells per coverslip. Cells were maintained in Neurobasal media supplemented with 0.5% penicillin/streptomycin, 2 mmol/l L-glutamine, 2% horse serum, and 2% B27 supplement. 50% media was changed every 48 hours. Transduction with scAAV9-GFP vectors was carried out at 40–48 hours after initial plating (2 days *in vitro*) by applying up to 5×10^9 vg per cell monolayer for 7 days before fixing in 4% paraformaldehyde. Cells were monitored on a daily basis, as GFP fluorescence was developed.

Immunocytochemistry

Transduced or mock-treated cells were fixed in 4% paraformaldehyde, permeabilized in 0.2% Triton X-100/PBS (PBS-Tx), blocked with 10% normal goat serum (NGS) in PBS-Tx and then incubated with primary antibodies in a single antibody staining assay against neuronal tubulin marker MAP2 (1:1,000; Sigma), motor neuron markers Islet-1 (1:1,000; Abcam, Cambridge, UK) or astrocyte marker GFAP (1:1,000; Sigma) diluted in 2% NGS/PBS-Tx overnight at 4 °C. The following day the cells were counter-stained with secondary Alexa-Fluor conjugated antibodies for 1 hour at room temperature, and washed in PBS between the incubations. Finally, coverslips were stained with Hoechst stain (1:2,000; Sigma) to visualize the nuclei and mounted onto a slide using FluoroMount media (Sigma). The images were captured on Leica confocal laser-scanning microscope using 63× oil lens and appropriate optical zoom, and processed using LAS AF Lite and ImageJ softwares.

Quantification of *in vitro* GFP fluorescence and statistical analysis

To quantify GFP-positive cells and intensity of GFP fluorescence, images were captured on InCell imager (GE Healthcare, Chalfont St Giles, UK) using 20× magnification. For determining transduction efficiencies using automated

Table 1 Primers used in construction of scAAV-GFP plasmids with different promoter elements

Primer name	*Sequence*	*Promoter construct*
Hb9A-Mlu For	GCGGCGG**ACGCG**TTGAATAAATTTAAGCAGG	Hb9cmv and Hb9e
Hb9A-Bgl Rev	GTATGC**AGATCT**AGCCCCATCCCCCTTCAAT	Hb9cmv and Hb9e
Hb9B-Bgl For	GCGCGG**AGATCT**AGAGTGGTTAGCTGATGAAT	Hb9cmv and Hb9e
Hb9B-Age Rev	CGTCTT**ACCGGT**TCTAATCAG CCTGCCTAGCT	Hb9cmv
Hb9B-Eco Rev	CGTCTT**GAATTC**TCTAATCAG CCT GCCTAGCT	Hb9e
CMVmp-Age For	GTAATG**AACCGG**TTAGGCGTGTACGGTGGGA	Hb9cmv
CMV Mlu For	GGCCGG**ACGCGT**GGA GCTAGTTATTAATAG	CMV
CMV-Eco Rev	ATTCGT**GAA TTC**AGG CTGGATCGGTCCCGGT	Hb9cmv and CMV
SYN1-Mlu For	ACAATG**ACGCGT**CTGCAGAGGGCCCTGCGTATG	SYN1
SYN1-Eco Rev	ATCATA**GAATTC**GCCGCAGCGCAGATGGTCGCG	SYN1
CAG Mlu For	ATTGGC**ACGCGT**GACATTGATTATTGACTA	CAG
CAG Eco Rev	ATTATT**GAATTC**CGCCCGCCGCGCGCTTCG	CAG

Primer hybridization sites are underlined. Sequences are demonstrated as 5′→3′. Restriction sites are highlighted in bold. Hb9A and B refer to 313 and 125 bp fragments, respectively. For, forward primer; Rev, reverse primer.

InCell Developer Software (GE Healthcare) with a gray level range of 0-65535, up to 3,000 cells were counted. Background GFP fluorescence was determined on cell-free area of each treatment or mock-treated cells, and the GFP-positive cell numbers were normalized to above the background values. In order to determine and compare GFP expression intensities for each treatment, the gray values in the GFP-positive cells above the background were averaged. The collected data represent mean values based on triplicate treatments. Statistical analysis of *in vitro* AAV transduction data was performed by one-way analysis of variance in GraphPad Prism (version 6.05) with each promoter representing a separate group. Multiple comparisons between the means were done using Tukey's multiple comparison test with 95% confidence interval.

In vivo scAAV9 transduction of wild-type neonatal mice

All experiments involving mice were conducted according to the Animal (Scientific Procedures) Act 1986, under Project License 40/3739 and approved by the University of Sheffield Ethical Review Sub-Committee, and the UK Animal Procedures Committee (London, UK). The UK Home Office code of practice for the housing and care of animals used in scientific procedures was followed according to Animal (Scientific Procedures) Act 1986. Animals were maintained in a controlled facility in a 12-hour dark/12-hour light cycle, a standardized room temperature of 21 °C, with free access to food and water.

For scAAV9 delivery into the CSF via cisterna magna, 15 wild-type C57BL/6 mice (n = 3 per group) at postnatal day 1 were anesthetized in an induction chamber using 5% isoflurane and oxygen at 3 l/minute before being placed on a red transilluminator (Philips Healthcare "Wee Sight"—product no. 1017920) with their head tilted slightly forward and nose attached to an anesthetic supply. Anesthesia was maintained with 2% isoflurane and oxygen at 0.3 l/minute. A 33-gauge needle attached to a Hamilton syringe and peristaltic pump was lowered approximately 1 mm into the cisterna magna area using stereotaxic apparatus at an angle of 45 degrees, and 1 µl of viral solution (1×10^{10} vg/µl) was injected at a rate of 1 µl/minute. An equal volume of PBS/35 mmol/l NaCl was used as a control solution. Three weeks after virus injection, the animals were terminally anesthetized with an intraperitoneal injection of an overdose of sodium pentobarbital, and perfused transcardially with PBS/heparin solution, followed by 4% paraformaldehyde (PFA) in PBS. Brains and spinal cords were postfixed in 4% PFA overnight at 4 °C, and then subjected to two rounds of cryoprotection by incubating the tissue in 30% sucrose/PBS solution for 24–48 hours at 4 °C.

Immunohistochemistry of CNS tissue

For immunohistochemistry analysis, the tissues were embedded in O.C.T. embedding matrix, and 40-µm-thick brain sections and 25-µm-thick spinal cord sections were cut on a cryostat at −22 °C free-floating or onto a slide, respectively. Brain sections or spinal cord sections were washed twice with PBS, permeabilized in PBS/0.3% Triton X-100, blocked with 10% NGS in PBS/0.3% Triton X-100 solution for up to 3 hours, and incubated with primary antibodies diluted in 2% NGS in PBS/0.15% Triton X-100 overnight. Primary antibodies were a combination of rabbit anti-GFP (1:500; Life Technologies) with either of the following mouse antibodies: anti-NeuN (1:300; Millipore, Watford, UK) or anti-Calcitonin gene related peptide (CGRP) (1:500; Sigma). The following day, the sections were washed in PBS four times for up to 2 hours and incubated with secondary antibodies Alexa-Fluor anti-mouse 568 or anti-rabbit 488 (Life Technologies) diluted in 5% NGS/PBS for 1 hour. For visualizing nuclei, 1:2500 Hoechst stain (Sigma) in PBS was used. Images were captured on Leica confocal microscope using 40× oil lens and optical zoom, and were processed using LAS AF Lite software and ImageJ. Low-magnification images of the spinal cord sections were captured on Leica confocal microscope using 10× dry lens and 488 nm wavelength (FITC channel) only. Low-magnification images of the brain sections were captured using 2× and 4× lens on a Nikon fluorescent microscope.

Quantification of *in vivo* gene transfer and statistical analysis

For quantification of GFP-positive cells in the ventral horns of lumbar and cervical spinal cord sections, a Nikon fluorescent microscope with 20× lens was used to capture an image of the ventral horn from three sections (approximately 300 µm apart) of lumbar and cervical spinal cord per animal. The sum of GFP-positive cells in the three ventral horns per animal was used for analysis. The data was normalized to the CMV promoter in the cervical group region. Statistical analysis on the spinal cord counts was performed by two-way analysis of variance using GraphPad prism, with region and promoter as the two independent variables. For spinal cord data set, simple effects of promoters (CMV, CAG, and SYN1 only) were compared within each region (cervical or lumbar) using Tukey's multiple comparisons test to a control group CMV.

For quantification of the brain sections, wide-field fluorescence images were captured using a 10× lens. In each of the four chosen brain areas (cerebellum, hippocampal formation, midbrain, and motor cortex), one image per region per animal (representing a region of 1 mm^2) was captured and used for counting. The numbers of GFP-positive cells were counted manually with the assistance of ImageJ software (Cell Counter plug-in), by an observer blinded to vector treatment. The cell counts were normalized to the average of scAAV9-CMV-GFP-treated group for each brain region. Statistical analysis for the brain counts was performed using one-way analysis of variance with Bonferroni's multiple comparison test to CMV control.

ACKNOWLEDGMENTS

This work was supported by the European Research Council grant (GTNCTV – 294745). V.L. and M.A. designed the study and wrote the manuscript. V.L. performed the experimental work including plasmid design and cloning, viral vector preparation, and characterisation, all *in vitro* and *in vivo* analyses. K.E.L. provided assistance with tissue processing, analysis of the results, and editing of the manuscript; I.C. performed cisterna magna injections and assisted in animal perfusion and dissection. A.J.G. provided advice in the preliminary *in vivo* work design and Individual Study Plan preparation. The authors thank Jayanth Chandran for the useful comments on the manuscript, Pádraig Mulcahy and Bartosz Muszynski for the help in establishing scAAV9-production protocol, Ellen Bennett for animal work technical support, and Richard Mead for assistance with the InCell analysis software. The authors declare no conflict of interest.

REFERENCES

1. Dayton, RD, Wang, DB and Klein, RL (2012). The advent of AAV9 expands applications for brain and spinal cord gene delivery. *Expert Opin Biol Ther* **12**: 757–766.
2. Foust, KD, Nurre, E, Montgomery, CL, Hernandez, A, Chan, CM and Kaspar, BK (2009). Intravascular AAV9 preferentially targets neonatal neurons and adult astrocytes. *Nat Biotechnol* **27**: 59–65.
3. Foust, KD, Salazar, DL, Likhite, S, Ferraiuolo, L, Ditsworth, D, Ilieva, H *et al*. (2013). Therapeutic AAV9-mediated suppression of mutant SOD1 slows disease progression and extends survival in models of inherited ALS. *Mol Ther* **21**: 2148–2159.
4. Foust, KD, Wang, X, McGovern, VL, Braun, L, Bevan, AK, Haidet, AM *et al.* (2010). Rescue of the spinal muscular atrophy phenotype in a mouse model by early postnatal delivery of SMN. *Nat Biotechnol* **28**: 271–274.
5. Valori, CF, Ning, K, Wyles, M, Mead, RJ, Grierson, AJ, Shaw, PJ *et al.* (2010). Systemic delivery of scAAV9 expressing SMN prolongs survival in a model of spinal muscular atrophy. *Sci Transl Med* **2**: 35ra42.
6. Fu, H, Muenzer, J, Samulski, RJ, Breese, G, Sifford, J, Zeng, X *et al.* (2003). Self-complementary adeno-associated virus serotype 2 vector: global distribution and broad dispersion of AAV-mediated transgene expression in mouse brain. *Mol Ther* **8**: 911–917.
7. Gao, G, Vandenberghe, LH, Alvira, MR, Lu, Y, Calcedo, R, Zhou, X *et al.* (2004). Clades of Adeno-associated viruses are widely disseminated in human tissues. *J Virol* **78**: 6381–6388.
8. Gray, SJ, Matagne, V, Bachaboina, L, Yadav, S, Ojeda, SR and Samulski, RJ (2011). Preclinical differences of intravascular AAV9 delivery to neurons and glia: a comparative study of adult mice and nonhuman primates. *Mol Ther* **19**: 1058–1069.
9. Inagaki, K, Fuess, S, Storm, TA, Gibson, GA, Mctiernan, CF, Kay, MA *et al.* (2006). Robust systemic transduction with AAV9 vectors in mice: efficient global cardiac gene transfer superior to that of AAV8. *Mol Ther* **14**: 45–53.
10. Gholizadeh, S, Tharmalingam, S, Macaldaz, ME and Hampson, DR (2013). Transduction of the central nervous system after intracerebroventricular injection of adeno-associated viral vectors in neonatal and juvenile mice. *Hum Gene Ther Methods* **24**: 205–213.
11. Ayers, JI, Fromholt, S, Sinyavskaya, O, Siemienski, Z, Rosario, AM, Li, A *et al.* (2015). Widespread and efficient transduction of spinal cord and brain following neonatal AAV injection and potential disease modifying effect in ALS mice. *Mol Ther* **23**: 53–62.
12. Bucher, T, Colle, MA, Wakeling, E, Dubreil, L, Fyfe, J, Briot-Nivard, D *et al.* (2013). scAAV9 intracisternal delivery results in efficient gene transfer to the central nervous system of a feline model of motor neuron disease. *Hum Gene Ther* **24**: 670–682.
13. Gray, SJ, Nagabhushan Kalburgi, S, McCown, TJ and Jude Samulski, R (2013). Global CNS gene delivery and evasion of anti-AAV-neutralizing antibodies by intrathecal AAV administration in non-human primates. *Gene Ther* **20**: 450–459.
14. Samaranch, L, Salegio, EA, San Sebastian, W, Kells, AP, Bringas, JR, Forsayeth, J *et al.* (2013). Strong cortical and spinal cord transduction after AAV7 and AAV9 delivery into the cerebrospinal fluid of nonhuman primates. *Hum Gene Ther* **24**: 526–532.

15. Samaranch, L, Salegio, EA, San Sebastian, W, Kells, AP, Foust, KD, Bringas, JR *et al.* (2012). Adeno-associated virus serotype 9 transduction in the central nervous system of nonhuman primates. *Hum Gene Ther* **23**: 382–389.
16. Hinderer, C, Bell, P, Vite, CH, Louboutin, JP, Grant, R, Bote, E *et al.* (2014). Widespread gene transfer in the central nervous system of cynomolgus macaques following delivery of AAV9 into the cisterna magna. *Mol Ther Methods Clin Dev* **1**: 14051.
17. McCarty, DM, Fu, H, Monahan, PE, Toulson, CE, Naik, P and Samulski, RJ (2003). Adeno-associated virus terminal repeat (TR) mutant generates self-complementary vectors to overcome the rate-limiting step to transduction in vivo. *Gene Ther* **10**: 2112–2118.
18. Gray, SJ, Foti, SB, Schwartz, JW, Bachaboina, L, Taylor-Blake, B, Coleman, J *et al.* (2011). Optimizing promoters for recombinant adeno-associated virus-mediated gene expression in the peripheral and central nervous system using self-complementary vectors. *Hum Gene Ther* **22**: 1143–1153.
19. Zincarelli, C, Soltys, S, Rengo, G and Rabinowitz, JE (2008). Analysis of AAV serotypes 1-9 mediated gene expression and tropism in mice after systemic injection. *Mol Ther* **16**: 1073–1080.
20. McLean, JR, Smith, GA, Rocha, EM, Hayes, MA, Beagan, JA, Hallett, PJ *et al.* (2014). Widespread neuron-specific transgene expression in brain and spinal cord following synapsin promoter-driven AAV9 neonatal intracerebroventricular injection. *Neurosci Lett* **576**: 73–78.
21. Nathanson, JL, Yanagawa, Y, Obata, K and Callaway, EM (2009). Preferential labeling of inhibitory and excitatory cortical neurons by endogenous tropism of adeno-associated virus and lentivirus vectors. *Neuroscience* **161**: 441–450.
22. Kügler, S, Lingor, P, Schöll, U, Zolotukhin, S and Bähr, M (2003). Differential transgene expression in brain cells *in vivo* and *in vitro* from AAV-2 vectors with small transcriptional control units. *Virology* **311**: 89–95.
23. Kügler, S, Meyn, L, Holzmüller, H, Gerhardt, E, Isenmann, S, Schulz, JB *et al.* (2001). Neuron-specific expression of therapeutic proteins: evaluation of different cellular promoters in recombinant adenoviral vectors. *Mol Cell Neurosci* **17**: 78–96.
24. Garg, SK, Lioy, DT, Cheval, H, McGann, JC, Bissonnette, JM, Murtha, MJ *et al.* (2013). Systemic delivery of MeCP2 rescues behavioral and cellular deficits in female mouse models of Rett syndrome. *J Neurosci* **33**: 13612–13620.
25. Hioki, H, Kameda, H, Nakamura, H, Okunomiya, T, Ohira, K, Nakamura, K *et al.* (2007). Efficient gene transduction of neurons by lentivirus with enhanced neuron-specific promoters. *Gene Ther* **14**: 872–882.
26. Peviani, M, Kurosaki, M, Terao, M, Lidonnici, D, Gensano, F, Battaglia, E *et al.* (2012). Lentiviral vectors carrying enhancer elements of Hb9 promoter drive selective transgene expression in mouse spinal cord motor neurons. *J Neurosci Methods* **205**: 139–147.
27. Lee, SK, Jurata, LW, Funahashi, J, Ruiz, EC and Pfaff, SL (2004). Analysis of embryonic motoneuron gene regulation: derepression of general activators function in concert with enhancer factors. *Development* **131**: 3295–3306.
28. Arber, S, Han, B, Mendelsohn, M, Smith, M, Jessell, TM and Sockanathan, S (1999). Requirement for the homeobox gene Hb9 in the consolidation of motor neuron identity. *Neuron* **23**: 659–674.
29. Wilson, JM, Hartley, R, Maxwell, DJ, Todd, AJ, Lieberam, I, Kaltschmidt, JA *et al.* (2005). Conditional rhythmicity of ventral spinal interneurons defined by expression of the Hb9 homeodomain protein. *J Neurosci* **25**: 5710–5719.
30. Nakano, T, Windrem, M, Zappavigna, V and Goldman, SA (2005). Identification of a conserved 125 base-pair Hb9 enhancer that specifies gene expression to spinal motor neurons. *Dev Biol* **283**: 474–485.
31. Schuster, DJ, Dykstra, JA, Riedl, MS, Kitto, KF, Belur, LR, McIvor, RS *et al.* (2014). Biodistribution of adeno-associated virus serotype 9 (AAV9) vector after intrathecal and intravenous delivery in mouse. *Front Neuroanat* **8**: 42.
32. Haidet-Phillips, AM, Hester, ME, Miranda, CJ, Meyer, K, Braun, L, Frakes, A *et al.* (2011). Astrocytes from familial and sporadic ALS patients are toxic to motor neurons. *Nat Biotechnol* **29**: 824–828.
33. Rindt, H, Feng, Z, Mazzasette, C, Glascock, JJ, Valdivia, D, Pyles, N *et al.* (2015). Astrocytes influence the severity of spinal muscular atrophy. *Hum Mol Genet* **24**: 4094–4102.
34. McGivern, JV, Patitucci, TN, Nord, JA, Barabas, ME, Stucky, CL and Ebert, AD (2013). Spinal muscular atrophy astrocytes exhibit abnormal calcium regulation and reduced growth factor production. *Glia* **61**: 1418–1428.
35. Peters, O, Schipke, CG, Philipps, A, Haas, B, Pannasch, U, Wang, LP *et al.* (2009). Astrocyte function is modified by Alzheimer's disease-like pathology in aged mice. *J Alzheimers Dis* **18**: 177–189.
36. Karumbayaram, S, Novitch, BG, Patterson, M, Umbach, JA, Richter, L, Lindgren, A *et al.* (2009). Directed differentiation of human-induced pluripotent stem cells generates active motor neurons. *Stem Cells* **27**: 806–811.
37. Singh Roy, N, Nakano, T, Xuing, L, Kang, J, Nedergaard, M and Goldman, SA (2005). Enhancer-specified GFP-based FACS purification of human spinal motor neurons from embryonic stem cells. *Exp Neurol* **196**: 224–234.
38. Mingozzi, F and High, KA (2011). Therapeutic *in vivo* gene transfer for genetic disease using AAV: progress and challenges. *Nat Rev Genet* **12**: 341–355.
39. Niwa, H, Yamamura, K and Miyazaki, J (1991). Efficient selection for high-expression transfectants with a novel eukaryotic vector. *Gene* **108**: 193–199.
40. Lock, M, Alvira, M, Vandenberghe, LH, Samanta, A, Toelen, J, Debyser, Z *et al.* (2010). Rapid, simple, and versatile manufacturing of recombinant adeno-associated viral vectors at scale. *Hum Gene Ther* **21**: 1259–1271.

Supplementary Information accompanies this paper on the *Molecular Therapy—Methods & Clinical Development* website (http://www.nature.com/mtm)